Supplementary Information

Invariant surface glycoprotein 65 of *Trypanosoma brucei* is a complement C3 receptor

Supplementary Data Figures and Tables

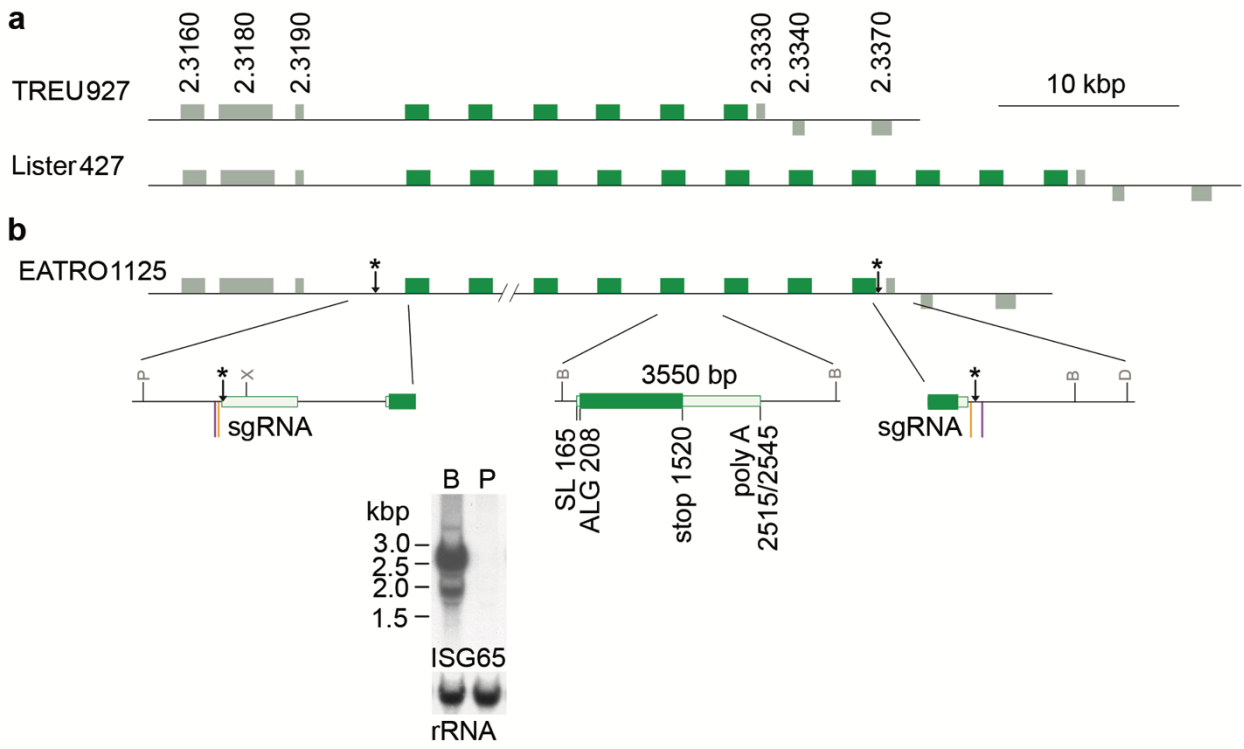

Supplementary Fig. 1: ISG65 loci and strategies to delete the locus

a. The ISG65 loci from the mosaic haploid genome sequences of *T. brucei* TREU927[24] and Lister 427[25]. ISG65 open reading frames are shown in green and others in grey. Boxes above the line indicate transcription from left to right and below the line from right to left. Open reading frames annotated in the genome but present within the 3'UTR of *ISG65* mRNA have been removed.
b. The upper panel shows a map of the ISG65 locus from *T. brucei* EATRO1125 derived from two cosmid clones. The break in the map represents the ends of the insert in the two cosmids and the number of missing ISG65 genes was not determined. Genes are indicated as in (A). The * symbols mark the ends of tandemly repeated ISG65 sequences. The location of the sgRNA is shown as an orange line and the 80 bp flanking sequence for insertion of the selectable marker cassette as a purple line. The lower panel shows a northern blot of total RNA from bloodstream (B) and procyclic (P) forms to show the size of the *ISG65* mRNA, n=1.

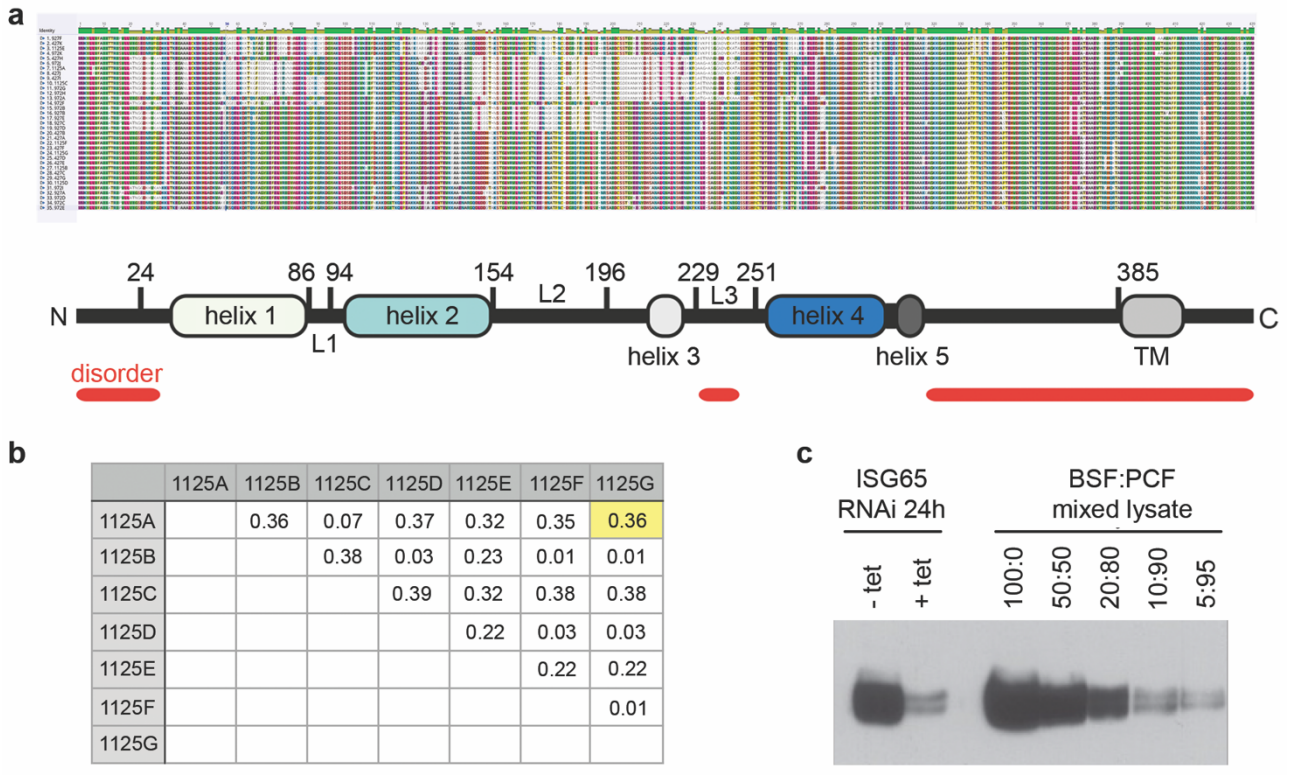

	1125A	1125B	1125C	1125D	1125E	1125F	1125G
1125A		0.36	0.07	0.37	0.32	0.35	0.36
1125B			0.38	0.03	0.23	0.01	0.01
1125C				0.39	0.32	0.38	0.38
1125D					0.22	0.03	0.03
1125E						0.22	0.22
1125F							0.01
1125G							

Supplementary Fig. 2: characterisation of ISG65 variation and knock-down

a. Alignment of polypeptide sequences of ISG65 from *T. brucei* EATRO1125 determined in this study and from the genome sequences of *T. brucei* TREU927 and Lister427 produced using Clustal Omega and using default settings in Geneious Prime 2021.2.2 (https://www.geneious.com). A larger scale alignment can be seen in Supplementary Fig. 8 and sequences are provided in “supplementary data 1.xlsx”. Below the alignment is a schematic of the structural features of ISG65, aligned against the sequence alignment. The red bars are regions predicted to be disordered as in Fig. 3. **b.** Difference matrix to show sequence identity between the ISG65 proteins from *T. brucei* EATRO1125 was prepared after a global alignment and Blosum 62 cost matrix via Geneious Prime 2021.2.2. The difference between ISG65A and G is highlighted in yellow. **c.** Western blot showing tetracycline-inducible depletion of ISG65 (n=1). *T. brucei* Lister427 pSPR2 p295 was grown in culture and RNAi induced for 24 h prior to analysing ISG65 knock down by western blotting. The same number of cell equivalents were loaded in each track. Comparison with standard curve of bloodstream form cells indicated there was ~90% depletion of ISG65 protein. These cells were used for immunofluorescence in Fig. 1b.

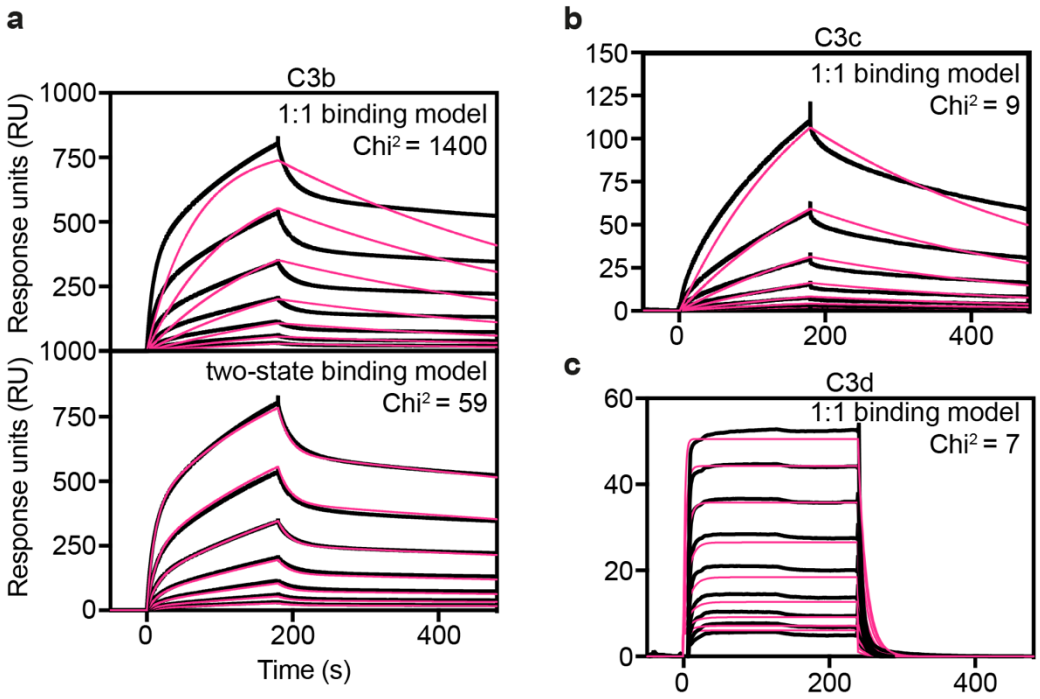

Supplementary Fig. 3: Surface plasmon resonance analysis of binding of C3 fragments to ISG65

ISG65G was immobilised on an SPR chip surface for assessment of binding of: **a.** C3b (a two-folding dilution series from a starting concentration of 0.5 μM); **b.** C3c (a two-folding dilution series from a starting concentration of 0.5 μM) and **c.** C3d (a two-folding dilution series from a starting concentration of 4 μM). Data was fitted to either a 1:1 binding model or a two-state binding model, as indicated, with the chi^2 for kinetic fitting reported, n=3.

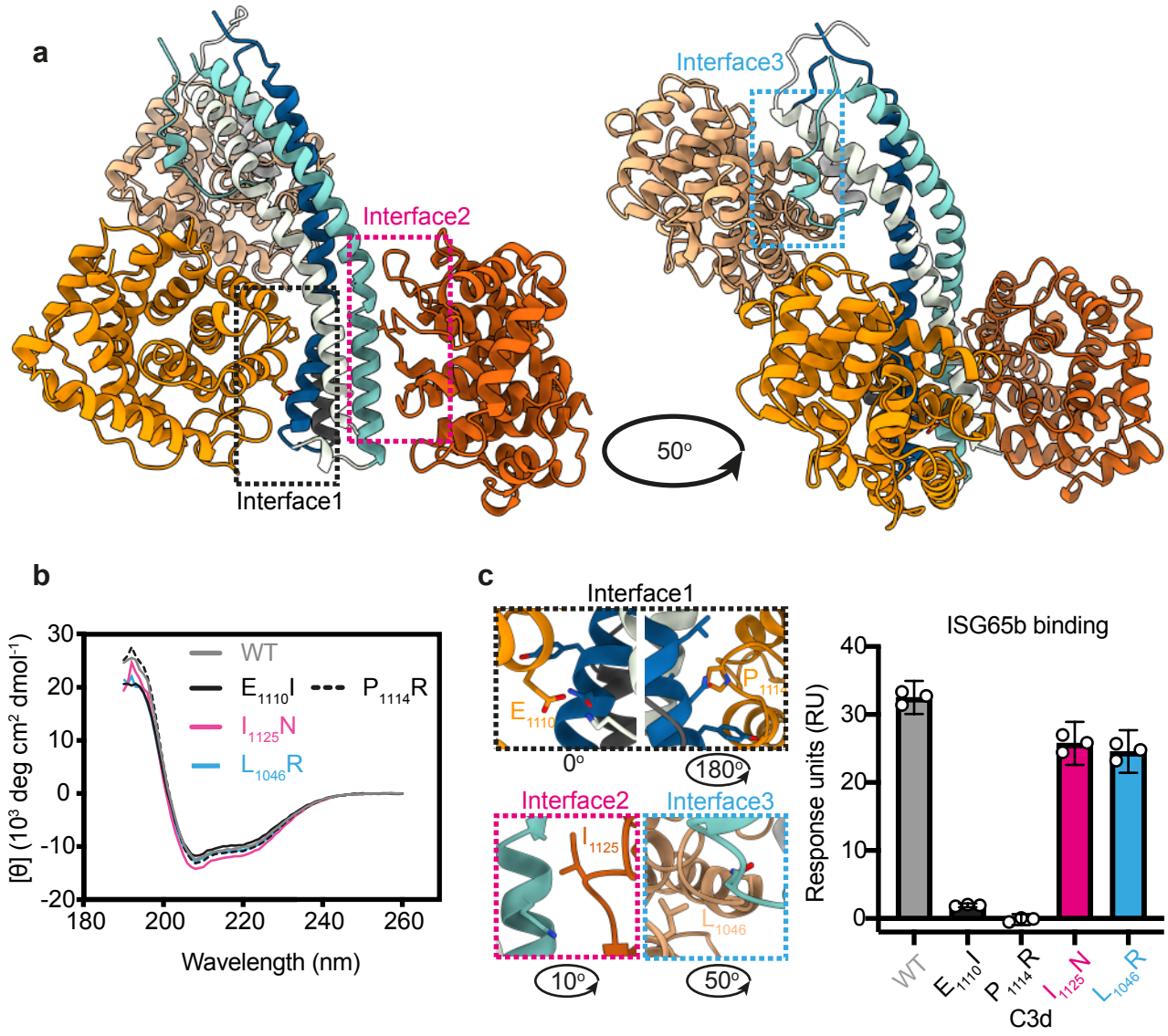

Supplementary Fig. 4: Determination of the ISG65-C3d interface

a. The crystal structure of ISG65-C3d revealed three possible interfaces between ISG65 and C3d. These were interface 1 (black box, orange C3d), interface 2 (pink box, dark orange C3d), and interface 3 (blue box, light orange C3d). **b.** Circular dichroism spectra of C3d and mutants designed to disrupt interface 1, 2, and 3. **c.** The left-hand panel shows close up views of the interfaces, coloured as **a.** and highlighting the mutations made to disrupt interfaces 1, 2, and 3. The right-hand panel shows the average binding of C3d and mutants to ISG65 (n = 3 technical replicates, with error bars denoting standard deviation) as measured by surface plasmon resonance analysis.

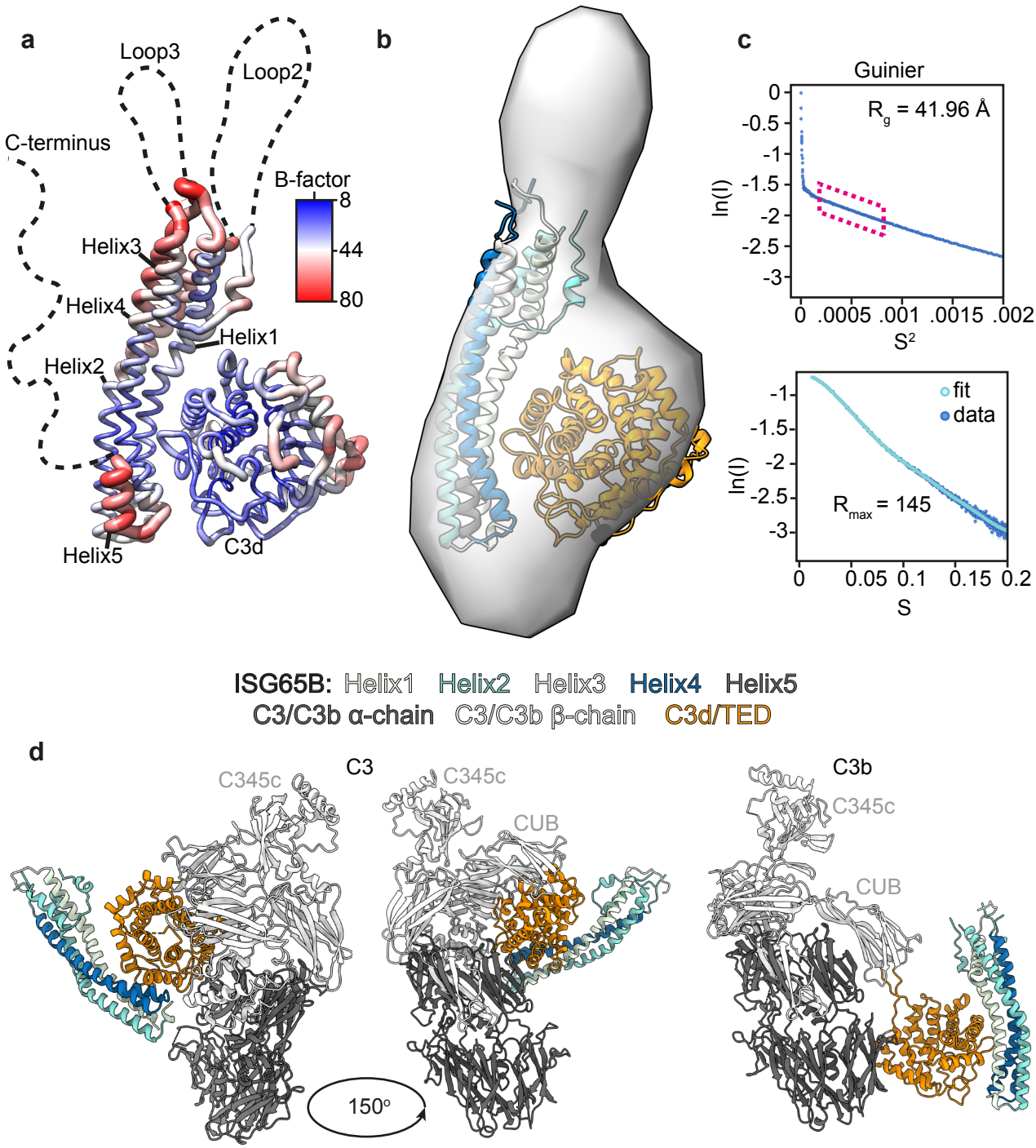

Supplementary Fig. 5: Analysis of the ISG65-C3d complex

a. The ISG65-C3d structure is shown as 'putty' with the width of the coil and the colour determined by B-factor. Dotted lines indicate the unresolved loops 2 and 3, and the C-terminal linker. **b.** The ISG65-C3d structure rigid body-fitted into the corresponding SAXS density. Initial fitting was performed using the Chimera fit_in_map tool[67] at a resolution of 15 Å, and then manually adjusted to account for the large density with no corresponding structure. This density is most likely attributable to loop L2. **c.** The top panel shows a Guinier plot of SAXS data, with a pink box showing the linear Guinier region used for fitting, and the resultant estimate of radius of gyration (R_g). The bottom panel shows SAXS data with corresponding fit and R_{max} value estimate, used for *ab initio* reconstruction of a 3D volume. Raw scattering curves are provided in "supplementary data 2". **d.** Models of ISG65 bound to complement C3 and C3b. The ISG65-C3d structure was docked onto structures of C3 (PDB: 2A73)[30] and C3b (PDB: 2I07)[9], with the light chain in light grey and the heavy chain in dark grey.

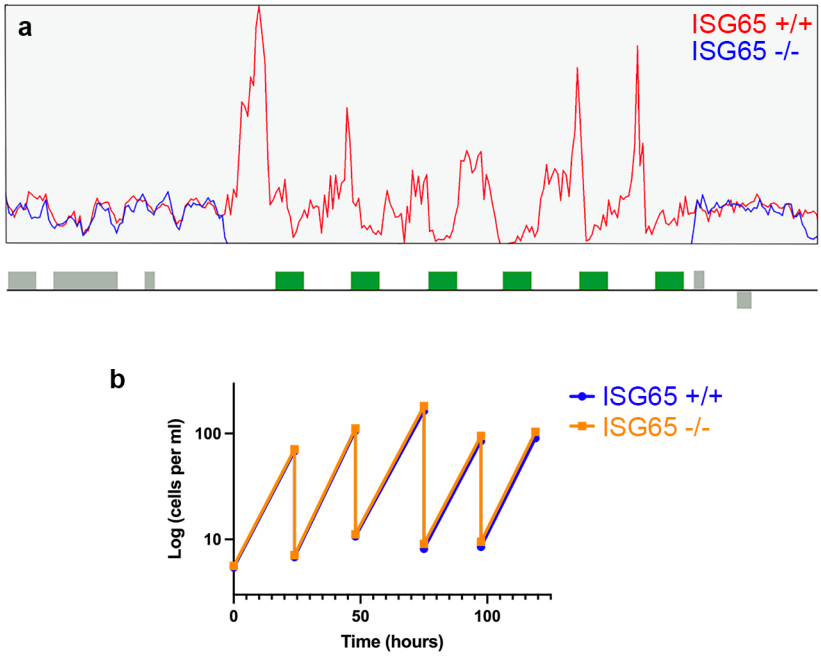

Supplementary Fig. 6: confirmation of ISG65 knockout in cell lines and assessment of its growth in culture

a. Mapping of sequencing reads from parental (red) and ISG65 knock-out (blue) cell lines onto the *T. brucei* TREU927 reference genome. ISG65 open reading frames are shown in green and others in grey. Boxes above the line indicate transcription from left to right and below the line from right to left. **b.** Growth in culture of *T. brucei* EATRO1125 ISG65+/+ (blue) and ISG65-/- (orange). Cells were passaged each day for 5 days.

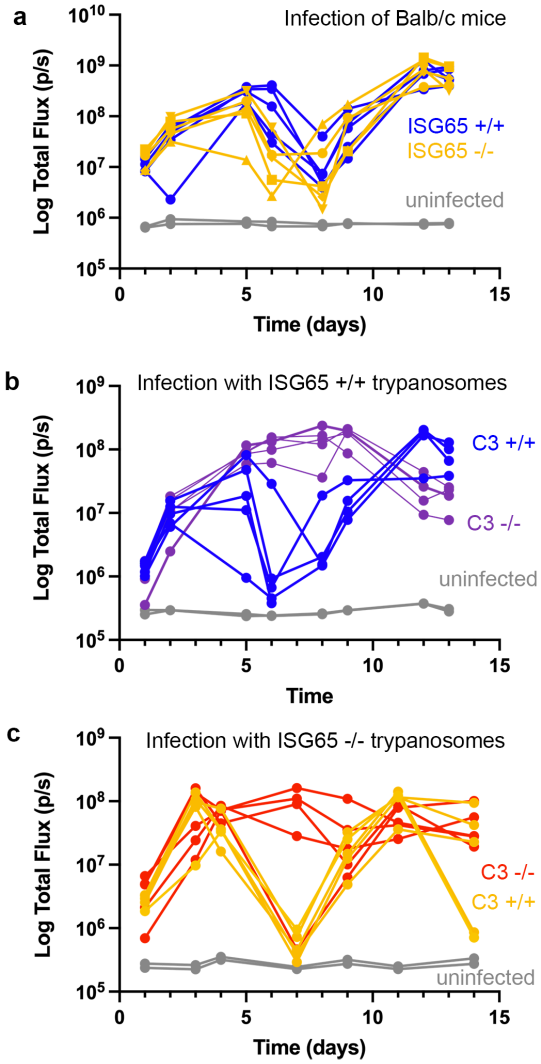

Supplementary Fig. 7: Assessment of the effect of ISG65 and C3 knock-out on trypanosome growth in mice

a. The effect of ISG65 knock-out on trypanosome infections in Balb/c mice. Five mice were infected with bioluminescent ISG65+/+ (blue, n=5 mice) or ISG65-/- (orange, n=5 mice) *T. brucei* cell lines. Two uninfected mice were used as controls for basal bioluminescence (grey, n=2 mice). Trypanosome burden was measured by imaging bioluminescence over time. **b.** The effect of C3 knock out on trypanosome infections in C57BL/6 mice. Bioluminescent ISG65+/+ *T. brucei* were used to infect five C57BL/6 mice (blue, n=5 mice) and five C57BL/6 mice lacking C3 (purple, n=5 mice). Two uninfected mice were used as controls for basal bioluminescence (grey, n=2 mice). Trypanosome burden was measured by imaging bioluminescence over time. **c.** The effect of C3 knock out on ISG65-/- trypanosome infections in C57BL/6 mice. Bioluminescent ISG65-/- *T. brucei* were used to infect five C57BL/6 mice (orange, n=5 mice) and five C57BL/6 mice lacking C3 (red, n=5 mice). These two infections were not done in parallel. Two uninfected mice were used as controls for basal bioluminescence (grey, n=2 mice). Trypanosome burden was measured by imaging bioluminescence over time. The data presented in Fig. 4a and 4b. were conducted concurrently, while that presented in Fig. 4c was conducted subsequently and should not be directly compared with the data in Fig 4a and 4b.

Supplementary Fig. 8: Alignment of ISG65 proteins analysed in this study

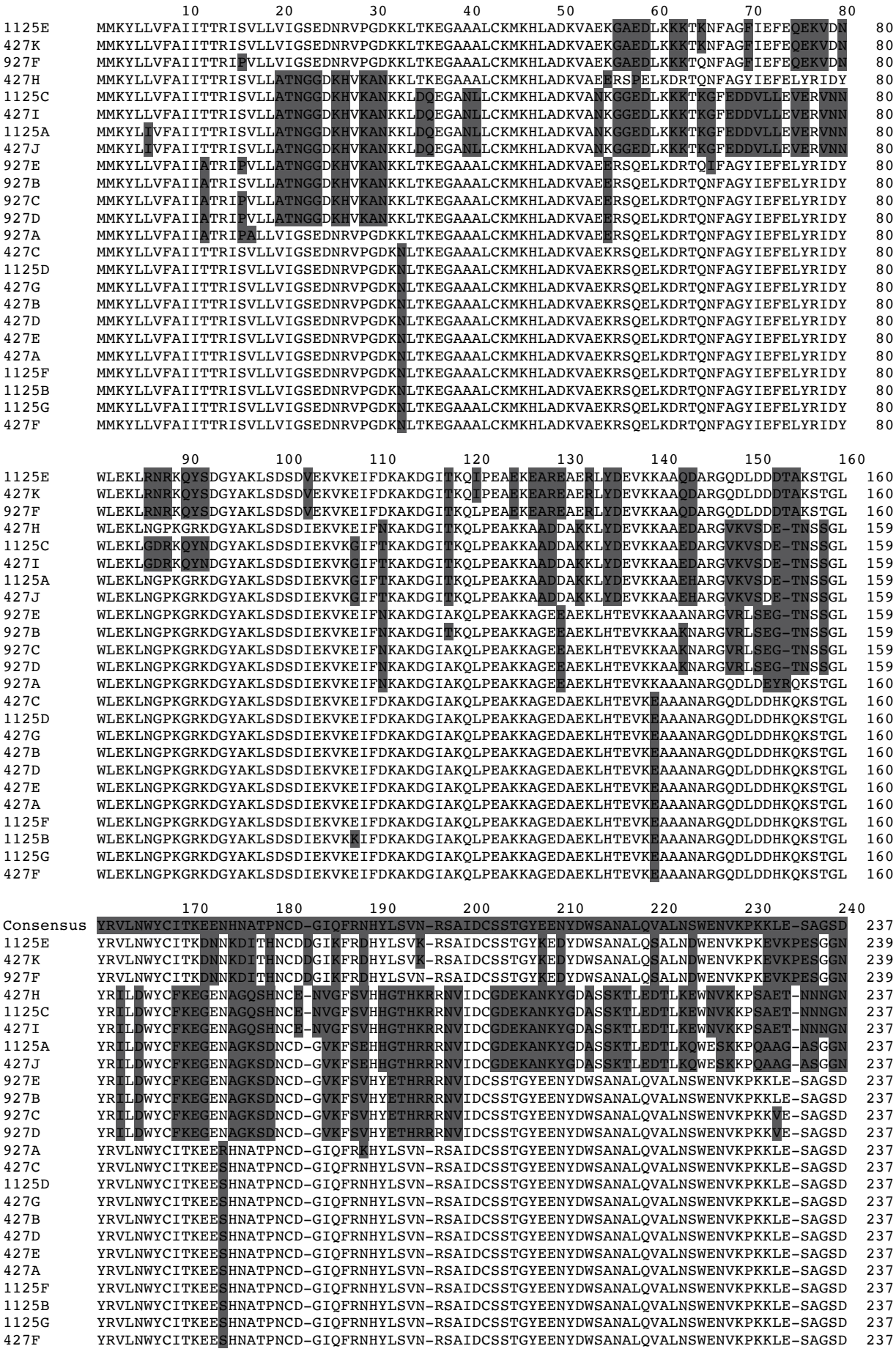

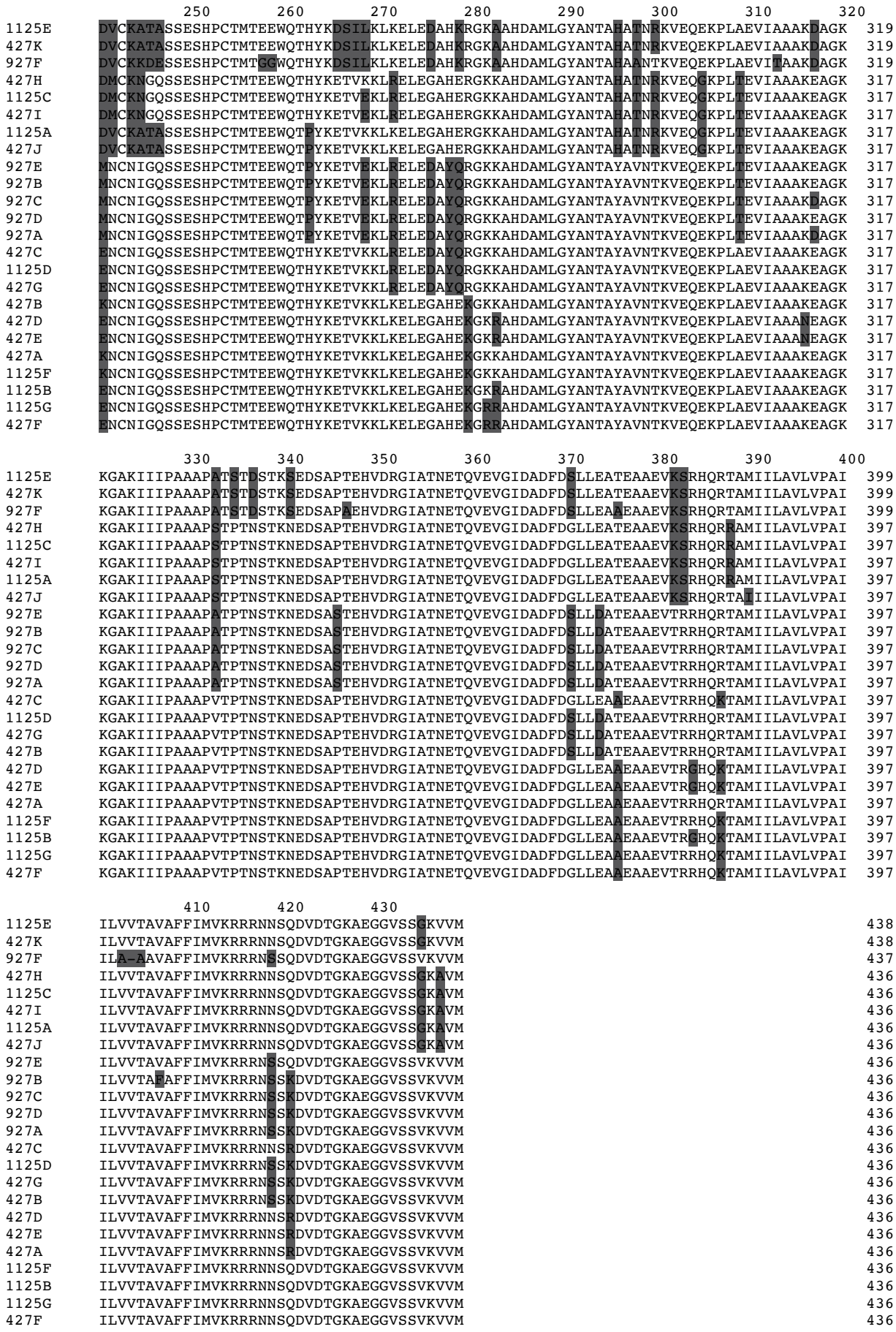
250 260 270 280 290 300 310 320
1125E DVCKATASSESHPCTMTEEWQTHYKDSILKLKELEDAHKRGKAAHDAMLGYANTAHATNRKVEQEKPLAEVIAAAKDAGK 319
427K DVCKATASSESHPCTMTEEWQTHYKDSILKLKELEDAHKRGKAAHDAMLGYANTAHATNRKVEQEKPLAEVIAAAKDAGK 319
927F DVCKKDESSESHPCTMTGGWQTHYKDSILKLKELEDAHKRGKAAHDAMLGYANTAHAANTKVEQEKPLAEVITAAKDAGK 319
427H DMCKNGQSSESHPCTMTEEWQTHYKETVKKLRELEGAHERGKKAHDAMLGYANTAHATNRKVEQGKPLTEVIAAAKEAGK 317
1125C DMCKNGQSSESHPCTMTEEWQTHYKETVEKLRELEGAHERGKKAHDAMLGYANTAHATNRKVEQGKPLTEVIAAAKEAGK 317
427I DMCKNGQSSESHPCTMTEEWQTHYKETVEKLRELEGAHERGKKAHDAMLGYANTAHATNRKVEQGKPLTEVIAAAKEAGK 317
1125A DVCKATASSESHPCTMTEEWQTPYKETVKKLKELEGAHERGKKAHDAMLGYANTAHATNRKVEQGKPLTEVIAAAKEAGK 317
427J DVCKATASSESHPCTMTEEWQTPYKETVKKLKELEGAHERGKKAHDAMLGYANTAHATNRKVEQGKPLTEVIAAAKEAGK 317
927E MNCNIGQSSESHPCTMTEEWQTPYKETVEKLRELEDAYQRGKKAHDAMLGYANTAYAVNTKVEQEKPLTEVIAAAKEAGK 317
927B MNCNIGQSSESHPCTMTEEWQTPYKETVEKLRELEDAYQRGKKAHDAMLGYANTAYAVNTKVEQEKPLTEVIAAAKEAGK 317
927C MNCNIGQSSESHPCTMTEEWQTPYKETVEKLRELEDAYQRGKKAHDAMLGYANTAYAVNTKVEQEKPLTEVIAAAKDAGK 317
927D MNCNIGQSSESHPCTMTEEWQTPYKETVEKLRELEDAYQRGKKAHDAMLGYANTAYAVNTKVEQEKPLTEVIAAAKEAGK 317
927A MNCNIGQSSESHPCTMTEEWQTPYKETVEKLRELEDAYQRGKKAHDAMLGYANTAYAVNTKVEQEKPLTEVIAAAKDAGK 317
427C ENCNIGQSSESHPCTMTEEWQTHYKETVKKLRELEDAYQRGKKAHDAMLGYANTAYAVNTKVEQEKPLAEVIAAAKEAGK 317
1125D ENCNIGQSSESHPCTMTEEWQTHYKETVKKLRELEDAYQRGKKAHDAMLGYANTAYAVNTKVEQEKPLAEVIAAAKEAGK 317
427G ENCNIGQSSESHPCTMTEEWQTHYKETVKKLRELEDAYQRGKKAHDAMLGYANTAYAVNTKVEQEKPLAEVIAAAKEAGK 317
427B KNCNIGQSSESHPCTMTEEWQTHYKETVKKLKELEGAHEKGKKAHDAMLGYANTAYAVNTKVEQEKPLAEVIAAAKEAGK 317
427D ENCNIGQSSESHPCTMTEEWQTHYKETVKKLKELEGAHEKGKRAHDAMLGYANTAYAVNTKVEQEKPLAEVIAAANEAGK 317
427E ENCNIGQSSESHPCTMTEEWQTHYKETVKKLKELEGAHEKGKRAHDAMLGYANTAYAVNTKVEQEKPLAEVIAAANEAGK 317
427A KNCNIGQSSESHPCTMTEEWQTHYKETVKKLKELEGAHEKGKKAHDAMLGYANTAYAVNTKVEQEKPLAEVIAAAKEAGK 317
1125F KNCNIGQSSESHPCTMTEEWQTHYKETVKKLKELEGAHEKGKKAHDAMLGYANTAYAVNTKVEQEKPLAEVIAAAKEAGK 317
1125B ENCNIGQSSESHPCTMTEEWQTHYKETVKKLKELEGAHEKGKRAHDAMLGYANTAYAVNTKVEQEKPLAEVIAAAKEAGK 317
1125G ENCNIGQSSESHPCTMTEEWQTHYKETVKKLKELEGAHEKGRRAHDAMLGYANTAYAVNTKVEQEKPLAEVIAAAKEAGK 317
427F ENCNIGQSSESHPCTMTEEWQTHYKETVKKLKELEGAHEKGRRAHDAMLGYANTAYAVNTKVEQEKPLAEVIAAAKEAGK 317
330 340 350 360 370 380 390 400
1125E KGAKIIIPAAAPATSTDSTKSEDSAPTEHVDRGIATNETQVEVGIDADFDSLLEATEAAEVKSRHQRTAMIILAVLVPAI 399
427K KGAKIIIPAAAPATSTDSTKSEDSAPTEHVDRGIATNETQVEVGIDADFDSLLEATEAAEVKSRHQRTAMIILAVLVPAI 399
927F KGAKIIIPAAAPATSTDSTKSEDSAPAEHVDRGIATNETQVEVGIDADFDSLLEAAEAAEVKSRHQRTAMIILAVLVPAI 399
427H KGAKIIIPAAAPSTPTNSTKNEDSAPTEHVDRGIATNETQVEVGIDADFDGLLEATEAAEVKSRHQRRAMIILAVLVPAI 397
1125C KGAKIIIPAAAPSTPTNSTKNEDSAPTEHVDRGIATNETQVEVGIDADFDGLLEATEAAEVKSRHQRRAMIILAVLVPAI 397
427I KGAKIIIPAAAPSTPTNSTKNEDSAPTEHVDRGIATNETQVEVGIDADFDGLLEATEAAEVKSRHQRRAMIILAVLVPAI 397
1125A KGAKIIIPAAAPSTPTNSTKNEDSAPTEHVDRGIATNETQVEVGIDADFDGLLEATEAAEVKSRHQRRAMIILAVLVPAI 397
427J KGAKIIIPAAAPSTPTNSTKNEDSAPTEHVDRGIATNETQVEVGIDADFDGLLEATEAAEVKSRHQRTAIIILAVLVPAI 397
927E KGAKIIIPAAAPATPTNSTKNEDSASTEHVDRGIATNETQVEVGIDADFDSLLDATEAAEVTRRHQRTAMIILAVLVPAI 397
927B KGAKIIIPAAAPATPTNSTKNEDSASTEHVDRGIATNETQVEVGIDADFDSLLDATEAAEVTRRHQRTAMIILAVLVPAI 397
927C KGAKIIIPAAAPATPTNSTKNEDSASTEHVDRGIATNETQVEVGIDADFDSLLDATEAAEVTRRHQRTAMIILAVLVPAI 397
927D KGAKIIIPAAAPATPTNSTKNEDSASTEHVDRGIATNETQVEVGIDADFDSLLDATEAAEVTRRHQRTAMIILAVLVPAI 397
927A KGAKIIIPAAAPATPTNSTKNEDSASTEHVDRGIATNETQVEVGIDADFDSLLDATEAAEVTRRHQRTAMIILAVLVPAI 397
427C KGAKIIIPAAAPVTPTNSTKNEDSAPTEHVDRGIATNETQVEVGIDADFDGLLEAAEAAEVTRRHQKTAMIILAVLVPAI 397
1125D KGAKIIIPAAAPVTPTNSTKNEDSAPTEHVDRGIATNETQVEVGIDADFDSLLDATEAAEVTRRHQRTAMIILAVLVPAI 397
427G KGAKIIIPAAAPVTPTNSTKNEDSAPTEHVDRGIATNETQVEVGIDADFDSLLDATEAAEVTRRHQRTAMIILAVLVPAI 397
427B KGAKIIIPAAAPVTPTNSTKNEDSAPTEHVDRGIATNETQVEVGIDADFDSLLDATEAAEVTRRHQRTAMIILAVLVPAI 397
427D KGAKIIIPAAAPVTPTNSTKNEDSAPTEHVDRGIATNETQVEVGIDADFDGLLEAAEAAEVTRGHQKTAMIILAVLVPAI 397
427E KGAKIIIPAAAPVTPTNSTKNEDSAPTEHVDRGIATNETQVEVGIDADFDGLLEAAEAAEVTRGHQKTAMIILAVLVPAI 397
427A KGAKIIIPAAAPVTPTNSTKNEDSAPTEHVDRGIATNETQVEVGIDADFDGLLEAAEAAEVTRRHQRTAMIILAVLVPAI 397
1125F KGAKIIIPAAAPVTPTNSTKNEDSAPTEHVDRGIATNETQVEVGIDADFDGLLEAAEAAEVTRRHQKTAMIILAVLVPAI 397
1125B KGAKIIIPAAAPVTPTNSTKNEDSAPTEHVDRGIATNETQVEVGIDADFDGLLEAAEAAEVTRGHQKTAMIILAVLVPAI 397
1125G KGAKIIIPAAAPVTPTNSTKNEDSAPTEHVDRGIATNETQVEVGIDADFDGLLEAAEAAEVTRRHQKTAMIILAVLVPAI 397
427F KGAKIIIPAAAPVTPTNSTKNEDSAPTEHVDRGIATNETQVEVGIDADFDGLLEAAEAAEVTRRHQKTAMIILAVLVPAI 397
410 420 430
1125E ILVVTAVAFFIMVKRRRNNSQDVDTGKAEGGVSSGKVVM 438
427K ILVVTAVAFFIMVKRRRNNSQDVDTGKAEGGVSSGKVVM 438
927F ILA-AAVAFFIMVKRRRNSSQDVDTGKAEGGVSSVKVVM 437
427H ILVVTAVAFFIMVKRRRNNSQDVDTGKAEGGVSSGKAVM 436
1125C ILVVTAVAFFIMVKRRRNNSQDVDTGKAEGGVSSGKAVM 436
427I ILVVTAVAFFIMVKRRRNNSQDVDTGKAEGGVSSGKAVM 436
1125A ILVVTAVAFFIMVKRRRNNSQDVDTGKAEGGVSSGKAVM 436
427J ILVVTAVAFFIMVKRRRNNSQDVDTGKAEGGVSSGKAVM 436
927E ILVVTAVAFFIMVKRRRNSSQDVDTGKAEGGVSSVKVVM 436
927B ILVVTAFAFFIMVKRRRNSSKDVDTGKAEGGVSSVKVVM 436
927C ILVVTAVAFFIMVKRRRNSSKDVDTGKAEGGVSSVKVVM 436
927D ILVVTAVAFFIMVKRRRNSSKDVDTGKAEGGVSSVKVVM 436
927A ILVVTAVAFFIMVKRRRNSSKDVDTGKAEGGVSSVKVVM 436
427C ILVVTAVAFFIMVKRRRNNSRDVDTGKAEGGVSSVKVVM 436
1125D ILVVTAVAFFIMVKRRRNSSKDVDTGKAEGGVSSVKVVM 436
427G ILVVTAVAFFIMVKRRRNSSKDVDTGKAEGGVSSVKVVM 436
427B ILVVTAVAFFIMVKRRRNSSKDVDTGKAEGGVSSVKVVM 436
427D ILVVTAVAFFIMVKRRRNNSRDVDTGKAEGGVSSVKVVM 436
427E ILVVTAVAFFIMVKRRRNNSRDVDTGKAEGGVSSVKVVM 436
427A ILVVTAVAFFIMVKRRRNNSRDVDTGKAEGGVSSVKVVM 436
1125F ILVVTAVAFFIMVKRRRNNSQDVDTGKAEGGVSSVKVVM 436
1125B ILVVTAVAFFIMVKRRRNNSQDVDTGKAEGGVSSVKVVM 436
1125G ILVVTAVAFFIMVKRRRNNSQDVDTGKAEGGVSSVKVVM 436
427F ILVVTAVAFFIMVKRRRNNSQDVDTGKAEGGVSSVKVVM 436

Supplementary Table 1: Mass spectrometry analysis identifies complement C3 as the ligand pulled down by ISG65

Pulldown samples were analysed by SDS-PAGE and a region of the gel containing two proteins unique to ISG65 were excised, as well as the corresponding region from a FHR pulldown from bovine serum as a control (Fig. 1c). Samples were trypsin-digested and analyzed by ESI-TRAP. All top hits are listed, except keratin which was removed from the list as a contaminant. This data is representative of two independent pulldowns and mass spectrometry analyses. Enrichment of proteins in ISG65 compared to FHR was performed.

ISG65 enriched or unique hits

Protein		MW	Peptides[2]	Coverage (%)[3]	Spectral counts[4]		Spectral index[5]		Ratio[6]
Accession #[1]	Description	(kDa)			ISG65	FHR	ISG65	FHR	ISG65/FHR
Q2UVX4	Complement C3	187.62	92	50.1	91.97	12.00	5.01^{-4}	4.78^{-5}	10.48
A6QPP2	SERPIND1 protein	55.32	6	12.9	1.00	n/a	3.38^{-7}	n/a	ISG65 only
G3N0V0	Uncharacterized protein	36.02	5	16.3	1.00	n/a	1.86^{-6}	n/a	ISG65 only
P06868	Plasminogen	91.42	4	4.2	2.97	n/a	2.78^{-6}	n/a	ISG65 only
F1MCF8	Uncharacterized protein	24.44	2	9.8	1.00	n/a	9.14^{-7}	n/a	ISG65 only
G5E5T5	Uncharacterized protein	42.55	3	8.2	1.00	n/a	1.26^{-6}	n/a	ISG65 only

[1]Accession number on UnitProt.
[2]Number of peptide sequences.
[3]Percent coverage of the protein with the found peptides.
[4]Spectral counts have been improved on the CPFP server by including fragment ion intensities in their caluation of [5]their spectral index.
[6]The spectral index is used to calculate the enrichment ratio. Complement C3 is enriched 10.5-fold in the ISG65 sample compared to the FHR sample.

Supplementary Table 2: ISG65 pulls down complement C3 from a broad spectrum of mammalian species

Pull-down samples the sera of various mammals were analysed by SDS-PAGE, and the most intense band excised for trypsin-digest mass spectrometry analysis (Figure 1d). The top hit from the corresponding species is listed, except keratin which was removed from the list as a contaminant.

Species	Accession #[1]	Description	Score	Peptides[2]	Coverage (%)[3]	PSM[4]
Human	P01024	Complement C3	1739	64	100	1015
Cow	Q2UVX4	Complement C3	1002	49	85	449
Horse	A0A3Q2HWQ6	Complement C3	158	11	17	102
Goat	A0A452DXE2	Complement C3	353	17	26	219
Dog	F1MCF8	Complement C3	845	46	87	715
Rabbit	P12247	Complement C3 alpha chain	105	21	17	96

[1]Accession number on UnitProt.
[2]Number of peptide sequences.
[3]Percent coverage of the protein with the found peptides
[4]Peptide spectrum matches

Supplementary Table 3: Kinetic parameters measured by surface plasmon resonance

Average values over three experimental repeats with corresponding standard deviation are displayed. For C3b and C3c, replicates were performed on three different flow paths with different immobilisation levels of ISG65. For C3d, replicates were performed on the same flow path.

	k_{a1} ($M^{-1}s^{-1}$)	k_{d1} (s^{-1})	k_{a2} (s^{-1})	k_{d2} (s^{-1})	K_D (nM)	Chi^2 (RU^2)
C3b	$9 \times 10^4 \pm 2 \times 10^4$	0.06 ± 0.009	0.01 ± 0.0004	0.001 ± 0.0005	67 ± 21	25 ± 25
C3c	$2 \times 10^4 \pm 1 \times 10^4$	0.008 ± 0.004	-	-	391 ±54	3.5 ± 3.9
C3d	$3 \times 10^5 \pm 7 \times 10^5$	0.1 ± 0.03	-	-	514 ± 90	5.2 ± 2.5

Supplementary Table 4: crystallographic statistics

Data collection	
Space group	$P12_11$
Cell dimensions:	
a, b, c (Å)	51.95, 189.58, 73.88
α, β, γ (°)	90.00, 90.11, 90.00
Resolution (Å)	94.79 – 2.6 (2.70-2.60)
Total observations	125,121 (13,131)
Total unique	43,218 (4392)
R_{pim}	0.165 (0.954)
$CC_{1/2}$	0.875 (0.31)
I/σ(I)	3.6 (0.7)
Completeness (%)	98.7 (96.4)
Multiplicity	2.9 (3.0)
Wilson B factor ($Å^2$)	41.0
Refinement	
Number of reflections	43141
R_{work} / R_{free}	0.2698 / 0.3100
Average B factor ($Å^2$)	51.0
Number of residues:	
Amino acid residues	996
Ligand molecules (GOL / PG0)	6
Waters	60
RMSZ deviations	
Bond lengths	0.007
Bond angles	0.900
Ramachandran plot	
Favoured (%)	96.4
Allowed (%)	3.5
Outliers (%)	0.1

Supplementary Table 5: Interactions between ISG65 and C3d

ISG65 residue	Atom	C3d residue	Atom
Hydrogen bonds			
D1174	OD2	Y70	OH
E1110	OE2	K84	NZ
E1110	OE2	N296	ND2
E1110	OE2	W81	NE1
E1110	OE2	Y80	OH
I1108	O	R77	NH2
K1111	O	Y293	OH
K1171	NZ	E74	OE2
L1109	O	R77	NH2
Q1112	O	R77	NH2
Q1112	O	R77	NH1
Q1119	OE1	Y293	OH
T1170	OG1	Y70	OH
Salt bridges			
K1171	NZ	E74	OE2
K1203	NZ	E59	OE1
E1110	OE2	K84	NZ
Residue-residue			
D1121		Q301	
D1121		T297	
E1110		N296	
E1110		Y293	
G1204		Y209	
I1108		F73	
K1111		Y293	
K1113		Y293	
K1171		F73	
K1171		Y70	
L1109		F73	
L1109		R77	
L1109		W81	
L1109		Y76	
L1109		Y80	
P1114		A289	
P1114		L286	
P1114		N290	
P1114		N290	
P1114		Y293	
P1205		Y209	
Q1119		Y293	
R1201		R63	
S1164		F73	

Uncropped blots for supplementary figures

Uncropped blot of RNAi knockdown of ISG65 in supplementary figure 1b.

A northern blot probed for ISG65. For more information, see Supplementary Figure 1b

A northern blot probed for rRNA. For more information, see Supplementary Figure 1b

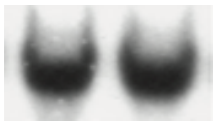

Uncropped blot of RNAi knockdown of ISG65 in supplementary figure 2c.

A Western blot using a polyclonal sera targeting ISG65 for detection. For more information, see Supplementary Figure 2c